JAIST Repository
https://dspace.jaist.ac.jp/

Title	Observation of Extremely High Current Densities on Order of MA/cm^2 in Copper Phthalocyanine Thin-Film Devices with Submicron Active Areas
Author(s)	Matsushima, Toshinori; Adachi, Chihaya
Citation	Japanese Journal of Applied Physics, 46(47): L1179-L1181
Issue Date	2007-11-30
Type	Journal Article
Text version	author
URL	http://hdl.handle.net/10119/7936
Rights	This is the author's version of the work. It is posted here by permission of The Japan Society of Applied Physics. Copyright (C) 2007 The Japan Society of Applied Physics. Toshinori Matsushima, and Chihaya Adachi, Japanese Journal of Applied Physics, 46(47), 2007, L1179-L1181. http://jjap.ipap.jp/link?JJAP/46/L1179/
Description	

Japan Advanced Institute of Science and Technology

Observation of Extremely High Current Densities on Order of MA/cm^2 in Copper Phthalocyanine Thin-Film Devices with Submicron Active Areas

Toshinori MATSUSHIMA[1] and Chihaya ADACHI[1,2]*

[1]*Core Research for Evolutional Science and Technology Program, Japan Science and Technology Agency, 1-32-12 Higashi, Shibuya, Tokyo 150-0011, Japan*

[2]*Center for Future Chemistry, Kyushu University, 744 Motooka, Nishi, Fukuoka 819-0395, Japan*

Using contact photolithography and electron-beam lithography techniques, we manufactured copper phthalocyanine thin-film devices with active areas ranging from 1,000,000 to 0.04 μm^2 to investigate how much current can flow through these devices with the aim of fabricating electrically pumped organic laser diodes. From the results of our current density-voltage (*J*-*V*) measurements, we found that the device with the smallest active area of 0.04 μm^2 on a silicon substrate exhibits an extremely high current density of 6,350,000 A/cm^2 due to improved thermal management. The *J*-*V* characteristics of the devices are controlled by shallow-trap space-charge-limited current (SCLC), trap-free SCLC, and two-carrier injection current mechanisms over a wide range of current densities between nA/cm^2 and MA/cm^2.

KEYWORDS: copper phthalocyanine, space-charge-limited current, electron-beam lithography, high-current-density injection, electrically pumped organic laser diode

*E-mail address: adachi@cstf.kyushu-u.ac.jp

Recently, organic thin-film devices, such as organic light-emitting diodes, have been developed due to their advantages for realizing low-cost, lightweight, flexible, large-area displays, and illumination applications.[1] Although studies on current density-voltage (J-V) characteristics are being conducted on these devices to determine their basic current flow mechanisms,[1-3] the current flow mechanisms have not been fully clarified to date. However, a more detailed understanding of these mechanisms is required for the development of future organic optoelectronic devices. In addition to these devices, which utilize current densities on the order of nA/cm^2 to A/cm^2, interest in high-current-density injection over kA/cm^2 is growing with the aim of determining the current flow mechanisms in a high-current-density region as well as fabricating electrically pumped organic laser diodes (OLDs).[4-9] Although the breakdown current densities of typical organic thin-film devices are as low as $\approx$ 10 A/cm^2, a high current density of at least 3.8 kA/cm^2 is required for the realization of OLDs.[4] For transporting such high current densities in organic thin films, it has been demonstrated that a decrease in active area (A) and the use of high-thermal-conductivity substrates are very effective in terms of heat management during device operation.[5-14] In this work, we fabricated copper phthalocyanine (CuPc) thin-film devices, and varied the active area of the devices from 1,000,000 to 0.04 μm^2 to demonstrate high-current-density injection in

the devices and to investigate the current flow mechanisms of the devices in a high-current-density region.

In our previous studies, we varied A from 1,000,000 to 7.9 μm^2 by forming holes in the insulating resist layer by contact photolithography.[7-9] However, contact photolithography limited the smallest value of A to 7.9 μm^2; therefore, in this study, we used electron-beam (EB) lithography to create smaller values of A.

We fabricated the CuPc devices, whose structure is shown in Fig. 1(a), according to the following steps. An EB resist film (ZEP-520A, Nippon Zeon Co.) was formed on a glass or silicon substrate coated with a 100-nm-thick indium tin oxide (ITO) anode layer with a sheet resistance of 25 Ω/sq by spin coating it at 6000 rpm for 30 s. After prebaking the film at 110ºC for 300 s, the film was transferred to an EB lithography chamber (ELIONIX ELS-7700H, Hitachi Co.) to engrave a square pattern (1 x 1, 0.5 x 0.5, or 0.2 x 0.2 μm) on the film. Then, the film was developed in ZED-N50 developer (Nippon Zeon Co.) for 300 s, rinsed in ZMD-B solution (Nippon Zeon Co.) for 60 s, and postbaked at 110ºC for 180 s. The substrate was plasma-etched in an SPK-202T RF magnetron chamber (Tokki Co.) for 40 s at 10 W under an oxygen flow of 10 cm^3/min to remove residual resist components on the ITO surface inside the holes. A 25-nm-thick CuPc active layer and a 200-nm-thick MgAg (Mg/Ag = 10/1 by weight) alloy cathode

layer[15] were vacuum-deposited on the holes at evaporation rates of 0.3 nm/s for CuPc and 0.33 nm/s for MgAg. Since the EB resist layer had good insulating characteristics (6.3×10^{-15} S·cm), current flow was confirmed to take place only through the holes. We fabricated the CuPc devices with A larger than 7.9 μm^2 using our previous contact photolithography technique for comparison.[7-9] The room-temperature J-V characteristics of the devices were measured using a semiconductor parameter analyzer (E5250A, Agilent Technologies) under a direct current.

We measured the thermally stimulated current (TSC) spectra of the CuPc devices using a TSC spectrometer (TSC-FETT EL2000, Rigaku Co.) to investigate hole traps in the CuPc films. The device was cooled to 80 K using liquid nitrogen. At 80 K, the device was biased with J = 5 mA/cm^2 for 2 min to fill the traps with injected holes. Then, the device was heated to room temperature at a heating rate (β) of 0.16 K/s. As the temperature increased, holes were released from the traps and the hole current was measured using a femtoammeter. Details of our TSC measurement conditions have been described in ref. 16.

Optical micrographs of the holes formed in the EB resist layer are shown in Figs. 1(b)-1(d). The slight blurring of these micrographs is due to the resolution limitation of optical microscopy. Since the EB lithography equipment has the ability to generate

submicron-area patterns precisely, perfectly square holes should be formed in the resist layer. We used the areas of 1, 0.25, and 0.04 μm^2, assuming square holes, to calculate the current densities of our devices. The expected error in current density, which originates from the estimation of the hole areas, was $< \pm$ 50%.

We obtained unique *J*-*V* characteristics featuring three distinct steps and extremely high current densities on the order of MA/cm^2 in the CuPc devices (Fig. 2). The maximum current density (J_{MAX}) and voltage (V_{MAX}) of each device is summarized in Table I. The largest device, with an active area of 1,000,000 μm^2 on a glass substrate had the smallest J_{MAX} of 7.6 A/cm^2 at a V_{MAX} of 5.0 V. J_{MAX} markedly increased from 7.6 to 3,640,000 A/cm^2 as the *A* was decreased from 1,000,000 to 0.04 μm^2. In addition, a high-thermal-conductivity silicon substrate provided a higher J_{MAX} than a low-thermal-conductivity glass substrate. The thermal conductivities of glass and silicon substrates are 1.1 and 148 W/(m·K), respectively. The J_{MAX} value of the CuPc device with A = 0.04 μm^2 on the silicon substrate was 6,350,000 A/cm^2 at a V_{MAX} of 16.9 V, which is the highest value ever reported for organic thin films. To confirm reproducibility, a large number of CuPc devices with A = 0.04 μm^2 were fabricated on different silicon substrates in separate vacuum preparations of CuPc, and the shapes of the *J*-*V* curves for the CuPc devices were exactly the same as those in Fig. 2, although

J_{MAX} slightly varied between 4.17 and 8.73 MA/cm^2.

Catastrophic device breakdowns under high-current operation are attributed to the melting of organic layers caused by Joule heat,[5-14] limiting J_{MAX} and V_{MAX}. Small active areas and high-thermal-conductivity substrates suppress the temperature increase inside the devices due to the effective removal of Joule heat from the organic layer to the surrounding heat sinks, e.g., the resist layer and substrate. Hence, smaller-area devices with a high-thermal-conductivity silicon substrate can sustain a higher-current-density operation than larger-area devices with a low-thermal-conductivity glass substrate.

Investigating the *J-V* characteristics of small-area organic devices with high current densities is useful for clarifying their carrier transport mechanisms in a high-current-density region. We supposed that the *J-V* characteristics of our devices were controlled by the following hole transport mechanisms. Mahapatro *et al*. reported that the ITO/CuPc interface allows ohmic hole injection.[17] When the devices were biased above the flat-band condition to cause carrier injection, the current abruptly increased at ≈ 1 V. Above this voltage, the *J-V* characteristics were controlled by a shallow-trap space-charge-limited current (SCLC) mechanism with the presence of traps at a discrete energy level [region (I) in Fig. 2], which is given by $J = (9/8) \cdot \varepsilon_r \cdot \varepsilon_0 \cdot \mu_h \cdot \theta \cdot (V^2/L^3)$,[2] where ε_r is the relative permittivity, ε_0 is the vacuum

permittivity, μ_h is the hole mobility, θ is the ratio of the free-hole to trapped-hole concentration, and L is the anode-cathode spacing. After traps were filled with injected holes at ≈ 6 V, the J-V characteristics were controlled by a trap-free SCLC mechanism [region (II) in Fig. 2], which is given by $J = (9/8) \cdot \varepsilon_r \cdot \varepsilon_0 \cdot \mu_h \cdot (V^2/L^3)$.[2] When we used ε_r = 3.6,[18] $\mu_h = 6.2 \times 10^{-2}$ cm^2/(V·s), and the θ values shown in Fig. 2, we obtained the best fitting between the J-V characteristics and these model equations (the solid lines in Fig. 2).

We also observed higher current densities than the trap-free SCLC [region (III) in Fig. 2]. Since the two-carrier injection of electrons and holes can provide higher current densities than the single-carrier injection of either electrons or holes,[2] the J-V characteristics in this region were probably controlled by a two-carrier injection current mechanism, which is given by $J = (125/18) \cdot \varepsilon_r \cdot \varepsilon_0 \cdot \tau \cdot \mu_h \cdot \mu_e \cdot (V^3/L^5)$,[2] where τ is the common average lifetime for injected electrons and holes and μ_e is the electron mobility. Since the J-V characteristics in region (III) were well described by a cubic law, we speculate that electron injection from the MgAg contacts starts at ≈10 V, and the transition from the trap-free SCLC to the two-carrier injection current occurs at this voltage.

The TSC spectra of the CuPc devices are shown in Fig. 3. Unfortunately, we could not obtain TSC spectra of the devices with A smaller than 10,000 μm^2 because the number of trapped holes was smaller for the smaller devices. The TSC spectrum area markedly decreased as A decreased. For TSC measurements, the hole-trap depth (d_t) and concentration (N_t) were calculated using $d_t = k \cdot T \cdot \ln(T^4/\beta)$ and $N_t = Q/(q \cdot A \cdot L)$, respectively, where k is the Boltzmann constant, T is the temperature at the TSC peak, Q is the total charge, which is identical to the area under the TSC peak, and q is the electronic charge.[16,19] These equations gave $d_t \approx 0.18$ eV and $N_t = 5.2 \times 10^{20}$ /cm^3 for A = 1,000,000 μm^2; $N_t = 1.6 \times 10^{20}$ /cm^3 for A = 250,000 μm^2; and $N_t = 4.9 \times 10^{19}$ /cm^3 for A = 40,000 μm^2. From these results, we attribute the large shift in the J-V characteristics in the shallow-trap SCLC region (I) in Fig. 2 to the change in hole-trap concentration in the CuPc layer. A similar shift in the J-V characteristics of CuPc devices was observed in our previous work.[5] We speculate that the change in the hole-trap concentration is due to the change in the CuPc grain structure, which is related to the carrier-trap concentration in the organic film.[20] Depositing hot MgAg on the CuPc layer causes a temperature increase in the CuPc layer, resulting in the change in the CuPc grain structure and an increase in the hole-trap concentration. The use of a small active area can control the temperature increase due to the removal of heat from the CuPc layer to

the resist layer. Therefore, smaller-area devices should have lower hole-trap concentrations than larger-area devices. Another possible explanation of this change is that CuPc molecules are partially decomposed by the temperature increase and the decomposed components act as hole traps in the CuPc layer.

We demonstrated that (1) CuPc devices with an active area of 0.04 μm^2 on a silicon substrate can transport an extremely high current density of 6,350,000 A/cm^2 due to improved thermal management, (2) the *J*-*V* characteristics of the CuPc devices are controlled by shallow-trap SCLC, trap-free SCLC, and two-carrier injection current mechanisms, and (3) a large shift in the *J*-*V* characteristics in the shallow-trap SCLC region is caused by the change in the hole-trap concentration in the CuPc layer. We emphasize that small-area devices with high current densities are useful for fabricating OLDs as well as for evaluating carrier transport mechanisms in a high-current-density region.

The authors are grateful to Professor Kuniharu Ijiro, Drs. Yoshihiko Tanamura, Kousei Ueno, and Michiaki Endo (Research Institute for Electronic Science, Hokkaido University) for technical support in electron-beam lithography.

References

1) S. R. Forrest: Nature (London) **428** (2004) 911.

2) M. A. Lampert and P. Mark: *Current Injection In Solids* (Academic Press, New York, 1970).

3) P. E. Burrows, Z. Shen, V. Bulovic, D. M. McCarty, S. R. Forrest, J. A. Cronin, and M. E. Thompson: J. Appl. Phys. **79** (1996) 7991.

4) . H. Yamamoto, T. Oyamada, H. Sasabe, and C. Adachi: Appl. Phys. Lett. **84** (2004) 1401.

5) H. Yamamoto, H. Kasajima, W. Yokoyama, H. Sasabe, and C. Adachi: Appl. Phys. Lett. **86** (2005) 083502.

6) B. Wei, M. Ichikawa, K. Furukawa, T. Koyama, and Y. Taniguchi: J. Appl. Phys. **98** (2005) 044506.

7) T. Matsushima, H. Sasabe, and C. Adachi: Appl. Phys. Lett. **88** (2006) 033508.

8) T. Matsushima and C. Adachi: Jpn. J. Appl. Phys. **46** (2007) L861.

9) T. Matsushima and C. Adachi: Proc. of SPIE, **6333** (2006) 63331O.

10) C. I. Wilkinson, D. G. Lidzey, L. C. Palilis, R. B. Fletcher, S. J. Martin, X. H. Wang, and D. D. C. Bradley: Appl. Phys. Lett. **79** (2001) 171.

11) N. Tessler, N. T. Harrison, and R. H. Friend: Adv. Mater. **10** (1998) 64.

12) N. T. Harrison, N. Tessler, C. J. Moss, K. Pichler, and R. H. Friend: Opt. Mater. **9** (1998) 178.

13) N. Tessler, N. T. Harrison, D. S. Thomas, and R. H. Friend: Appl. Phys. Lett. **73** (1998) 732.

14) D. J. Pinner, R. H. Friend, and N. Tessler: Synth. Met. **111** (2000) 257.

15) C. W. Tang and S. A. VanSlyke: Appl. Phys. Lett. **51** (1987) 913.

16) T. Matsushima, M. Yahiro, and C. Adachi: Appl. Phys. Lett. **91** (2007) 103505.

17) A. K. Mahapatro, N. Sarkar, and S. Ghosh: Appl. Phys. Lett. **88** (2006) 162110.

18) A. Sussman: J. Appl. Phys. **38** (1967) 2738.

19) Z. Fang, L. Shan, T. E. Schlesinger, and A. G. Milnes: Mater. Sci. Eng. B **5** (1990) 397.

20) A. D. Carlo, F. Piacenza, A. Bolognesi, B. Stadlober, and H. Maresch: Appl. Phys. Lett. **86** (2005) 263501.

Figure captions

Fig. 1. (a) Schematic structure of CuPc devices with small active areas. Optical micrographs of holes formed in insulating EB resist layer: (b) 1 x 1 μm, (c) 0.5 x 0.5 μm, and (d) 0.2 x 0.2 μm.

Fig. 2. *J*-*V* characteristics of CuPc devices with various active areas and substrates.

Fig. 3. TSC spectra of CuPc devices with various active areas on glass substrates.

Table I. Maximum voltage (V_{MAX}) and current density (J_{MAX}) for CuPc devices with various active areas and substrates.

A (μm^2)	Substrate	V_{MAX} (V)	J_{MAX} (A/cm^2)
1,000,000	Glass	5.0	7.6
250,000	Glass	5.5	26.7
40,000	Glass	5.9	96.2
10,000	Glass	5.8	296
2,500	Glass	3.7	314
625	Glass	3.7	574
117	Glass	5.3	2,290
34.6	Glass	6.4	23,200
7.9	Glass	9.2	128,000
1.0	Glass	10.8	432,000
0.25	Glass	11.7	1,800,000
0.04	Glass	14.1	3,640,000
0.04	Silicon	16.9	6,350,000

Toshinori Matsushima and Chihaya Adachi
Japanese Journal of Applied Physics

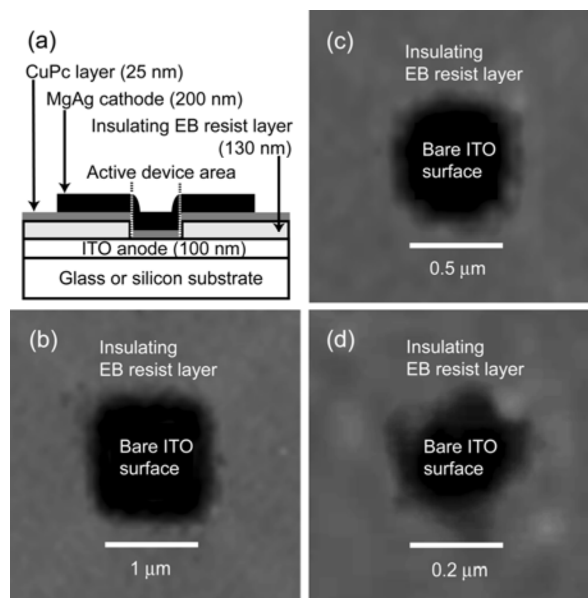

Fig. 1.

Toshinori Matsushima and Chihaya Adachi

Japanese Journal of Applied Physics

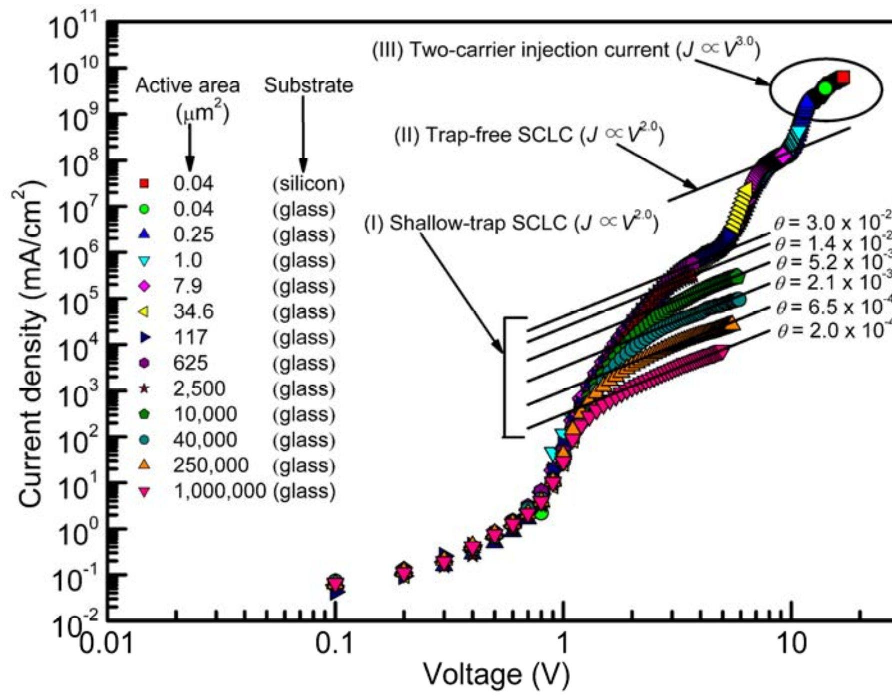

Fig. 2.

Toshinori Matsushima and Chihaya Adachi

Japanese Journal of Applied Physics

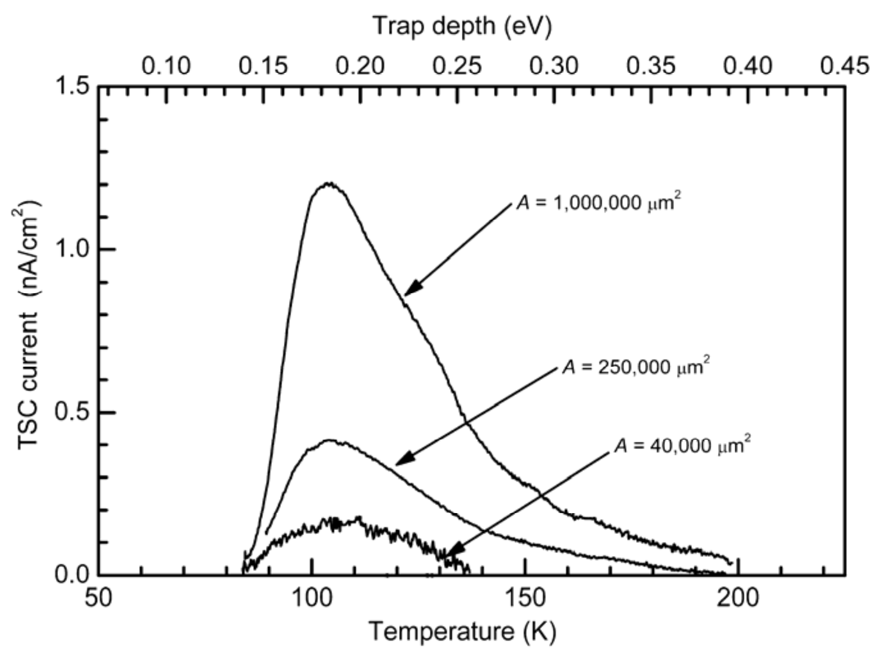

Fig. 3.

Toshinori Matsushima and Chihaya Adachi

Japanese Journal of Applied Physics